Available online at www.sciencedirect.com

ScienceDirect

journal homepage: www.elsevier.com/locate/he

Effect of hydrogen-diesel fuel co-combustion on exhaust emissions with verification using an in–cylinder gas sampling technique

Midhat Talibi[*], *Paul Hellier*, *Ramanarayanan Balachandran*, *Nicos Ladommatos*

Department of Mechanical Engineering, University College London, London, United Kingdom

ARTICLE INFO

Article history:
Received 30 April 2014
Received in revised form
4 July 2014
Accepted 9 July 2014
Available online 6 August 2014

Keywords:
Hydrogen
Combustion
Compression ignition engine
Gas sampling valve
NO_x formation
Particulate production

ABSTRACT

The paper presents an experimental investigation of hydrogen-diesel fuel co-combustion carried out on a naturally aspirated, direct injection diesel engine. The engine was supplied with a range of hydrogen-diesel fuel mixture proportions to study the effect of hydrogen addition (aspirated with the intake air) on combustion and exhaust emissions. The tests were performed at fixed diesel injection periods, with hydrogen added to vary the engine load between 0 and 6 bar IMEP. In addition, a novel in–cylinder gas sampling technique was employed to measure species concentrations in the engine cylinder at two in–cylinder locations and at various instants during the combustion process.

The results showed a decrease in the particulates, CO and THC emissions and a slight increase in CO_2 emissions with the addition of hydrogen, with fixed diesel fuel injection periods. NO_x emissions increased steeply with hydrogen addition but only when the combined diesel and hydrogen co-combustion temperatures exceeded the threshold temperature for NO_x formation. The in–cylinder gas sampling results showed higher NO_x levels between adjacent spray cones, in comparison to sampling within an individual spray cone.

Copyright © 2014, The Authors. Published by Elsevier Ltd on behalf of Hydrogen Energy Publications, LLC. This is an open access article under the CC BY-NC-ND license (http://creativecommons.org/licenses/by-nc-nd/3.0/).

Introduction

The ever-growing demand for energy has led to the increased popularity of compression-ignition (CI) engines due to their higher thermal efficiencies, relatively stable combustion characteristics, reliability and durability. However CI engines suffer from drawbacks of undesirably high emissions of nitrogen oxides (NO_x) and particulate matter (PM) [1]. Concerns over health effects and air quality have resulted in the imposition of stringent limits on pollutant emissions from CI engines around the world. This legislation, addressing both environmental and security of supply concerns, is designed to reduce the dependence on petroleum based fossil fuels, and has raised interest in the research and development of sustainable and cleaner burning fuels.

Hydrogen (H_2) is a 'zero' carbon fuel and therefore produces no particulate matter, total hydrocarbons (THC), carbon monoxide (CO) or carbon dioxide (CO_2) emissions from combustion [2]. However, hydrogen has an appreciably lower

* *Corresponding author*. Tel.: +44 20 7679 0012.
E-mail addresses: m.talibi@ucl.ac.uk, midhattalibi@hotmail.com (M. Talibi).
http://dx.doi.org/10.1016/j.ijhydene.2014.07.039
0360-3199/Copyright © 2014, The Authors. Published by Elsevier Ltd on behalf of Hydrogen Energy Publications, LLC. This is an open access article under the CC BY-NC-ND license (http://creativecommons.org/licenses/by-nc-nd/3.0/).

cetane number than diesel fuel [2] and is not ignitable merely by means of compression in modern diesel engines, and therefore it requires an ignition source. In the case of a diesel engine, the hydrogen can either be aspirated into the engine or injected directly into the cylinder, while the auto-ignition of diesel fuel spray can act as a pilot to ignite the hydrogen [3,4]. Hydrogen requires a very low amount of energy to ignite but has high flame propagation rates within the engine cylinder in comparison to hydrocarbon fuels, even at lean mixture conditions. The high flame speeds are a result of the fast and thermally neutral branching chain reactions of H_2 as compared to the relatively slower endothermic and thermally significant chain reactions associated with hydrocarbon fuel combustion [2].

Heat release rates from H_2-diesel fuel co-combustion tend to be higher than those for diesel fuel combustion, resulting in a shorter duration of combustion with less heat transfer to the surroundings, and can improve thermal efficiencies [5–7]. However, Masood et al. [6] and Christodoulou et al. [7] reported a small deterioration in thermal efficiency when operating the engine with a H_2-diesel fuel mixture, at low load and low speed conditions, which they attributed to the incomplete burning of all the hydrogen aspirated into the engine.

A considerable number of studies [3,5,7–9] reported a reduction in PM emissions when H_2 was used as a secondary fuel in a diesel engine, which they ascribed to a number of factors; firstly, increased oxidation of particulates due to higher in–cylinder temperatures that result from increased heat release rates, secondly the overall reduction in the carbon–hydrogen ratio of the combined H_2-diesel fuel, and thirdly the formation of OH radicals from H_2 combustion which also enhance PM oxidation. Tomita et al. [10] reported a reduction in smoke to near zero levels at all diesel injection timings and at all equivalence ratios of hydrogen. Tsolakis and Hernandez [1] used reformed exhaust gas recirculation (REGR) to introduce hydrogen rich gas to the engine intake air and reported a reduction in the total number and mass of PM emissions, but no effect was noted on the particle size distribution compared to standard diesel operation. Some investigators reported an increase in PM emissions at high engine loads [4,8]. When H_2 is aspirated into the engine via the engine inlet manifold, it displaces some of the intake air and can reduce the power density of the engine. At high load operating conditions, which are accompanied by high levels of H_2 substitution, the intake air becomes increasingly vitiated, slowing the rate of carbon oxidation reactions, which can result in a rise in PM emissions.

NO_x emissions have been reported to increase as stoichiometric H_2-air ratios are approached, and reach a peak value at an equivalence ratio of 0.9 [11,12]. The faster burning rates of H_2 relative to fossil diesel [5] and the resulting higher in–cylinder temperatures, especially when operating with near-stoichiometric H_2-air mixture conditions, has been suggested by some investigators to give rise to increased NO_x exhaust emissions [1,8]. Conversely, other investigators, such as Lambe and Watson [3] and Tomita et al. [10], have reported considerable reductions in NO_x emissions with H_2-diesel fuel co-combustion, at certain load conditions with relatively advanced diesel fuel injection timings. Saravanan et al. [5,9] conducted co-combustion experiments, at various engine loads, during which diesel fuel was replaced with H_2 while keeping the engine speed constant. Significant reductions in NO_x emission levels were observed, at low engine loads, when 30% of the initial volume of diesel fuel was replaced with H_2 in the intake air (keeping the engine speed constant), which these authors attributed to lean burn combustion. An 80% reduction in NO_x emissions was reported by Saravanan et al. [5,9], at high engine loads, with 90% of the diesel fuel volume replaced by hydrogen. At full load engine operating conditions, NO_x emissions were reported by Saravanan et al. to marginally increase. Lilik et al. [4] noted that the engine used by Saravanan et al. [5,9] produced NO_x at an order of a magnitude higher than usually emitted by modern diesel engines, and any decrease in NO_x could therefore be a result of enhanced turbulent in–cylinder mixing.

Masood et al. [6,13] carried out computational H_2-diesel fuel co-combustion studies and validated the findings against experimental results. Both the computational and experimental NO_x emission results showed an overall decrease in NO_x with increasing H_2 addition except for a marginal increase in NO_x reported in the experimental data at high H_2 substitution levels. The overall decrease in NO_x with increasing H_2 substitution was attributed to the increase in mole fraction of water vapour in the combustion products produced from H_2 combustion, absorbing energy released from combustion and reducing peak combustion temperatures.

Lilik et al. [4] substituted up to 15% of energy from diesel fuel by H_2 aspirated into the engine intake air. Two engine speeds (1800 rpm and 3600 rpm) and two engine loads (25% and 75% of the maximum output) were investigated, and while it was observed that the effect of H_2 substitution on NO_x emissions was minimal, a greater increase at low engine loads was reported compared to high engine loads with the addition of H_2. Considering only the NO component of the total NO_x emissions, increased H_2 substitution led to decreasing levels of NO emissions especially at low load. However, NO_2 emissions were observed to increase, when the ratio of H_2 in the intake charge was increased, most significantly at high engine load. This reduction in NO/NO_2 ratio was verified using numerical modelling and was attributed to the increased availability of the HO_2 radicals with increasing H_2 addition and subsequent reaction of HO_2 with NO. The numerical model also showed that the spatial temperature distribution in the cylinder was relatively unaffected by H_2 combustion, and it was therefore suggested that the observed changes in NO_x were not the result of changes in thermal NO. The authors attributed the small reduction in the overall NO_x emissions to the slight increase in ignition delay causing a small shift in the combustion phasing towards the expansion stroke and, therefore, generally lower in–cylinder gas temperatures.

More recently Christodoulou et al. [7] conducted H_2-diesel fuel co-combustion engine tests where up to 8% by volume of the intake air was replaced with hydrogen. At low load conditions, no significant changes in NO_x emissions were reported with the introduction of H_2, which was attributed to the smaller thermal boundary layer of the hydrogen flame and the relatively cooler engine walls which enhanced heat rejection and offset the higher adiabatic flame temperature of hydrogen. At higher load conditions and increasing

displacement of diesel fuel with H_2, NO_x emissions increased due to elevated flame temperatures.

The above review of literature suggests some lack of clarity as to the effect of H_2-diesel fuel co-combustion on NO_x emissions and also particulate emissions at high loads, with results of previous investigations being at times contradictory, particularly in the case of NO_x emissions.

The study reported in the current paper investigated the effects of co-combustion of diesel fuel with H_2 on exhaust emissions; H_2 addition in the engine ranged from low levels to predominantly H_2 combustion, with the function of diesel injection being only to ignite the H_2. The experiments reported here were conducted at a variety of engine loads. For all experiments, the H_2 was injected into the engine inlet manifold to be aspirated with the intake air. In a complimentary set of experiments, nitrogen gas was added to the engine intake air (instead of hydrogen) so as to isolate the effects of diluting the intake charge (reducing the amount of combustible oxygen). The paper also reports a series of experiments conducted using a timed in–cylinder sampling valve so as to analyse the burning gases in the engine cylinder at different instants during the combustion cycle.

Experimental setup

Engine facility

All the experiments were conducted on a naturally aspirated, single cylinder, high speed, direct injection, compression-ignition engine. The cylinder head (including the valves), the injection system and the piston were from a donor 2.0 L, 4-cylinder Ford Duratorq engine, and were mounted on a Ricardo Hydra crankcase to form a single-cylinder research engine. The geometry specifications for the engine are listed in Table 1. A piezoelectric pressure transducer (Kistler 6056A), installed via a glow plug adaptor, was used to measure the engine in–cylinder gas pressure every 0.2 CAD in conjunction with a Kistler 5018 charge amplifier. As the in–cylinder pressure transducer was of the piezoelectric type, it required reference to a known absolute pressure. This was accomplished by setting the in–cylinder pressure, at every engine cycle when the piston was at BDC, to the inlet manifold pressure which was measured with a Druck piezoresistive pressure transducer, installed 160 mm upstream of the inlet valves. These pressure readings, in addition to several control and operation temperatures, were logged by PCs utilizing National Instruments (NI) data acquisition systems. A bespoke NI LabVIEW program, developed in-house, post-processed the in–cylinder pressure data in order to evaluate the net apparent heat release rates and the indicated mean effective pressure (IMEP), utilizing a one dimensional and single zone thermodynamic model and assuming homogenous conditions and ideal gas behaviour [14].

Table 1 – Engine specifications.

Bore	86 mm
Stroke	86 mm
Swept volume	499.56 cm^3
Compression ratio (geometric)	18.3:1
Maximum in–cylinder pressure	150 bar
Piston design	Central ω – bowl in piston
Fuel injection pump	Delphi single-cam radial-piston pump
High pressure common rail	Delphi solenoid controlled, 1600 bar max.
Diesel fuel injector	Delphi DFI 1.3 6-hole solenoid valve injector
Electronic fuel injection system	1 μs duration control
Crank shaft encoder	1800 ppr, 0.2 CAD resolution
Full engine load (at 1200 rpm, 900 bar fuel injection pressure)	9 bar IMEP

The flow of air supplied to the naturally aspirated engine was measured using a Romet (G65) positive displacement volumetric air flow metre. Pressure and temperature measurements, taken immediately adjacent to the air flow metre inlet, were used to convert the volumetric air flow rate to air mass flow rate. The oil and coolant water were circulated around the engine head and crankcase at a temperature of 80 ± 2.5 °C. A six-hole (154 μm hole diameter) Delphi DFI 1.3 servo-hydraulic solenoid valve fuel injector was used for the direct injection of diesel fuel with the injection pressure, injection timing and duration controlled using an EmTronix engine control system (EC-GEN 500).

Hydrogen gas was supplied from a compressed hydrogen gas bottle and was injected into the engine inlet manifold 350 mm upstream of the inlet valves. The flow of H_2 was controlled using a Bronkhorst thermal mass flow controller (F-201-AV-70K), to an accuracy of ±0.08 L/min.

Analysis of gaseous exhaust emissions was performed with an exhaust gas analyser rack (Horiba MEXA-9100HEGR) housing a non-dispersive infrared absorption analyser for CO and CO_2 emissions, a chemiluminescence analyser for NO_x measurements, a flame ionization detector for THC emissions and a magneto-pneumatic analyser to measure oxygen concentrations. The exhaust particulate mass and size distribution were measured by a differential mobility spectrometer (Cambustion DMS500). Exhaust gas sample, for both the gaseous and particulate analysers, was taken 30 mm downstream of the exhaust valves and conveyed to the analysers via heated lines which were maintained at 190 °C and 80 °C for the measurement of gaseous and particulate compositions respectively.

Fig. 1 shows a schematic of the test engine setup, including hydrogen delivery.

In–cylinder gas sampling system

In–cylinder gas sampling techniques have been previously used by other investigators as a means to analyse the composition histories of stable species formed during the course of the combustion process inside the combustion chamber [15,16]. Often, the gas sampling system is timed so that the extraction of the gas sample from the cylinder can occur at a specific narrow crank angle window during the combustion process [15]. Recently, Nowak et al. [17] applied the gas sampling technique to understand the fuel oxidation mechanism in an engine by observing the change in species concentration during the compression and expansion strokes.

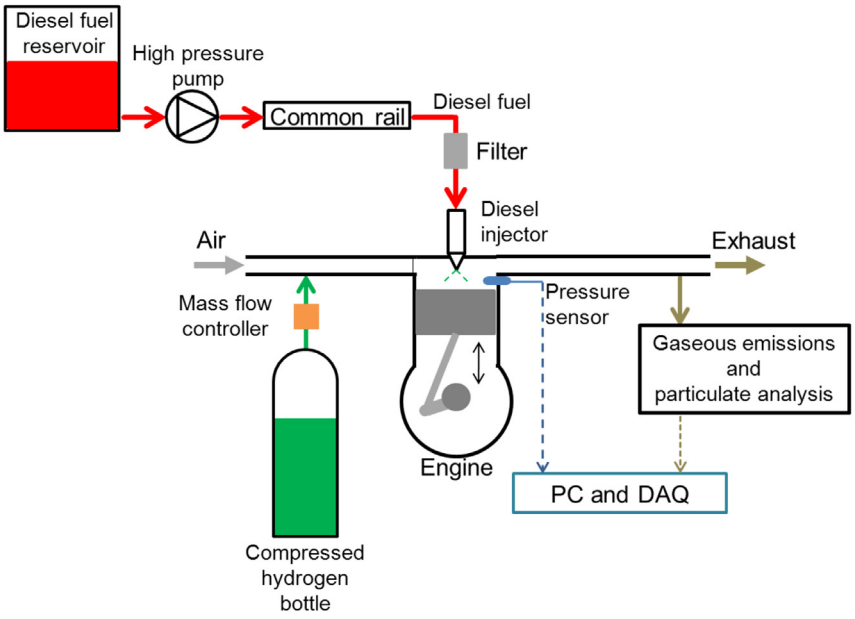

Fig. 1 – Schematic showing test engine arrangement including H_2 delivery and exhaust emissions instrumentation.

For the study reported in this paper, a novel in–cylinder gas sampling system, designed and commissioned in-house, was used. This included an intermittent, timed, high-speed, electromagnetically actuated, 'poppet-type' sampling valve [18] and a heated dilution tunnel. The sampling valve (Fig. 2) was based on the 'percussion' principle in which the electromagnetic armature is not connected directly to the valve stem. This allows shorter sampling durations (<1 ms), enabling the measurement of local, in–cylinder gas composition at any particular instant of the engine cycle to be resolved to a window of a few crank angle degrees (CAD). The electromagnet, when switched on, causes the armature to accelerate and travel at high speed towards the valve stem and impact the stem, imparting a force large enough to open the poppet valve very briefly (period of order 6-10 CAD), allowing a small sample of in–cylinder gas to flow from the engine cylinder into the valve. The poppet valve lift (of order 0–0.5 mm) was monitored with a sensitive LVDT displacement sensor (Kaman 1U1 probe), installed so as to sense the displacement of the stem of the sampling valve. The timing of the sampling valve was selectable with a resolution of 0.2 CAD, using an in-house built controller in conjunction with the crank-shaft encoder, so as to allow the sampling valve to be opened at any desired crank angle in the engine cycle.

The sampling valve was installed in the engine head in place of one of the two inlet valves. The sampling valve tip penetration into the combustion chamber could be varied from 0 mm (flush with the engine cylinder head) to a maximum penetration of 9 mm. Fig. 3 shows the relative positions of the diesel injector and the sampling valve inside the engine head with respect to the piston position at TDC.

The sampling valve was opened once every three engine cycles and the extracted in–cylinder gas samples were fed to a heated dilution tunnel, also designed and built in-house. The purpose of the heated dilution tunnel (maintained at 200 °C) was to buffer the gas samples and mix them with heated nitrogen gas (at 180 °C) to increase the volume of the sample sufficiently so that it could be measured by the Horiba gaseous emission analyser described in Section Engine facility. The undiluted and diluted gas sample streams were consecutively

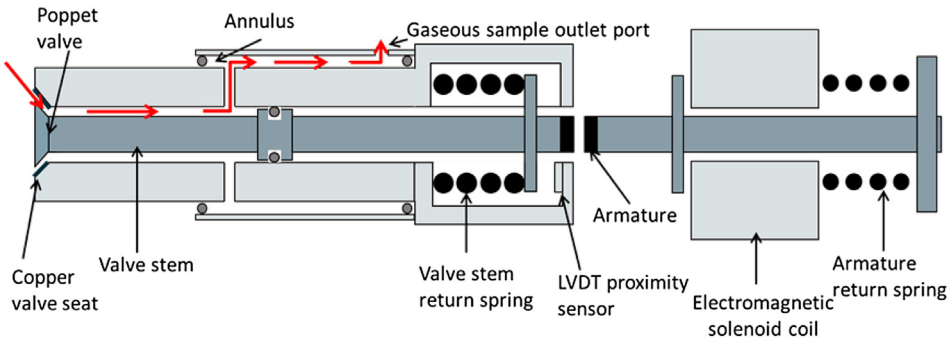

Fig. 2 – Simplified diagram of the in–cylinder sampling valve showing the gas flow from within the cylinder to the sample outlet port.

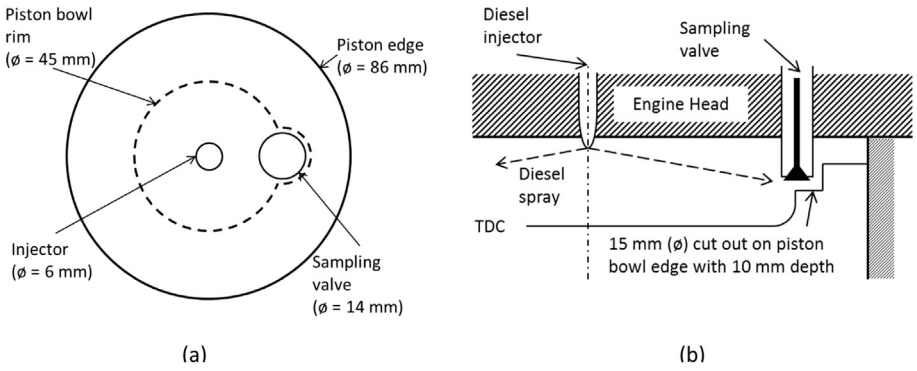

Fig. 3 – Schematic showing (a) plan view and (b) side view of the relative locations of the injector, the sampling valve at maximum in–cylinder penetration and the piston at TDC.

fed into a stand-alone CO_2 analyser (which can function with relatively much lower flow rates) and then passed to the emissions analyser rack (Horiba MEXA-9100EGR) respectively, and the mass ratio of the undiluted to the diluted in–cylinder gas sample was calculated by means of measured molar concentrations of CO_2 in the undiluted and diluted gas sample. The gas sample extracted from the engine cylinder passed through the sampling valve seat into the sampling passage, the length of which was about 3 orders of magnitude relative to the valve opening lift. It is, therefore, expected that the heat transfer from the gas sample to the valve seat, coupled with the expansion of the sample gas from the cylinder gas pressure (40–100 bar) to near atmospheric pressure, caused the sample gas temperature to drop rapidly, quenching any combustion reactions. Thus the composition of the sample gas measured by the analysers was assumed to be representative of the stable species in the combustion chamber that were extracted during the short sampling window. Using the equations formulated by Zhao and Ladommatos [18] to estimate the volume of an in–cylinder gas sample attaining a roughly hemispherical shape, a volume of 0.44 cm^3 was determined for a gas sample at an in–cylinder gas pressure of 64 bar (at 10 CAD ATDC) for the sampling valve utilised in the current study. This gas sample of volume 0.44 cm^3 represents about 1.6% of the combustion chamber volume at TDC for the 0.5 L/cylinder compression-ignition engine used in this study, which reduces to negligible levels as a percentage as the expansion stroke progresses.

Experimental procedure and fuels used

All the experiments were carried out at a constant engine speed of 1200 rpm, common-rail fuel injection pressure of 900 bar, and a diesel fuel injection timing of 10 CAD BTDC. The diesel injector had been previously calibrated so that the volume of diesel fuel injected per engine cycle could be determined from the duration of injection period. The diesel fuel injector calibration was carried out using a burette with which the volumetric flow rate of diesel fuel was determined, at steady state conditions, with different diesel fuel injection duration periods. Compressed hydrogen gas of 99.995% purity was obtained from a commercial gas supplier (BOC), while the diesel fuel used for all tests was of fossil origin with a cetane number of 53.2 and carbon to hydrogen ratio of 6.32:1. Table 3 shows further properties of diesel fuel and hydrogen.

Experimental set 1: exhaust emission tests

The adopted test procedure consisted of fixing the diesel fuel injection period (i.e. fixing the flow rate of diesel fuel supplied to the engine) while gradually increasing the H_2 supplied to the engine so as to increase the engine load (power output), at constant engine speed.

The above procedure was repeated for a range of fixed diesel fuel injection periods, as shown in Table 2. Fig. 4 shows the energy supplied to the single cylinder engine from H_2 as a percentage of the total energy supplied to the engine (energy from H_2 plus diesel fuel) and the concentration of H_2 in the intake air, at various engine loads and fixed diesel injection periods.

In the above set of tests, the minimum diesel fuel injection period used was 250 μs. With this injection period and no H_2 addition, no heat release could be discerned from the analysis of in–cylinder gas pressure. It is suggested that this may be attributable to diesel fuel-air mixture overleaning and thus unable to sustain a flame front and be more prone to

Table 2 – Test parameters used in the exhaust emission experiments.

Diesel fuel injection period (μs)	Diesel fuel flow per engine cycle ($\times 10^{-3}$ ml/engine cycle)	Diesel fuel-air equivalence ratio (φ_D)	Engine load with no H_2 addition (bar IMEP)	H_2 flow rate injected in inlet manifold ($\times 10^{-3}$ L/engine cycle)	H_2-air equivalence ratio (φ_H)
250	1.58	0.08	0.00	0 to 31.3	0 to 0.40
325	2.94	0.20	1.50	0 to 25	0 to 0.31
350	3.93	0.23	2.20	0 to 21.3	0 to 0.26
400	5.30	0.29	3.25	0 to 17.5	0 to 0.21

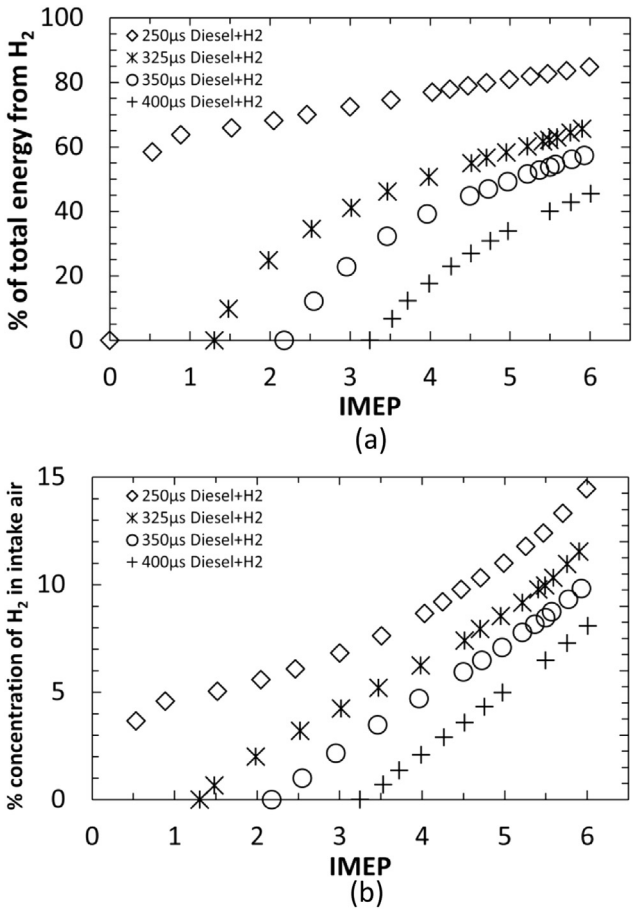

Fig. 4 – (a) Percentage energy from H_2 and (b) concentration of H_2 in the intake air at various engine loads and fixed diesel injection periods.

quenching by cooler areas of the in–cylinder charge. Therefore, 250 μs was taken to be the minimum diesel fuel injection period (at an injection pressure of 900 bar), as below this injection duration no discernable exhaust THC emissions could be observed, suggesting that injector opening was insufficient for delivery of diesel fuel. Nevertheless, it was observed that 250 μs diesel fuel injection period was sufficient to ignite the aspirated H_2-air mixture at all engine loads up to 6 bar IMEP.

An additional series of control tests were carried out using diesel fuel only (without any H_2), with the diesel fuel injection period varied so that the engine load changed between 0 and 6 bar IMEP.

Experimental set 2: in–cylinder gas sampling tests

A further set of experiments was carried out using the in–cylinder gas sampling valve; the diesel injection period was fixed at 325 μs for all the tests, as at this injection duration, and in the case of no H_2 addition to the engine-intake air, and an engine load of 1.5 bar IMEP was obtained, with only negligible levels of NO_x measured in the exhaust gases. Therefore, in the course of the in–cylinder sampling experiments, it could be assumed that any observed NO_x could be primarily attributed to the presence of H_2. Meanwhile, an engine load of 1.5 bar IMEP indicated that sufficient diesel fuel was being delivered at this diesel injection duration for the development of heat release from diesel only combustion, and that spatial differences in the in–cylinder charge attributable to the presence of diesel sprays could likely be observed during in–cylinder sampling.

During these tests, gas samples were extracted from the engine cylinder at two distinctly different locations, relative to one of the six injector nozzle diesel fuel sprays. Fig. 5 shows the two relative sampling arrangements with respect to the injector sprays. The first location, relative to the spray, was a region of high diesel fuel concentration within the core of the diesel fuel spray, while the second location, relative to the spray, was an area of relatively low diesel fuel concentration between two spray cones. Since the absolute location of the sampling valve in the engine head was fixed, the change in the sampling arrangement, relative to the diesel fuel sprays, was achieved through rotation of the centrally-located injector. The locations of relatively high and low diesel fuel concentration were experimentally determined by rotating the diesel fuel injector in small steps and measuring the in–cylinder gas composition (in particular levels of unburned hydrocarbons) at each injector rotation.

For each of the two relative sampling arrangements shown in Fig. 5, gas samples were extracted at three sampling windows in the engine cycle: (a) the premixed stage of combustion (10 CAD ATDC); (b) the early diffusion combustion stage (25 CAD ATDC); and (c) the late burning stage (40 CAD ATDC). Table 4 lists the timings and the durations, within the engine cycle, of the three sampling windows.

Table 3 – Properties of diesel fuel and hydrogen at 1 atm and 300 K [2,9].

Property	Diesel fuel	Hydrogen
Density (kg/m^3)	831.9	0.0838
Lower heating value (MJ/kg)	43.14	120

Results and discussion

Combustion characteristics

Fig. 6(a) shows the heat release rate curves at two engine loads, 3 and 6 bar IMEP, for both diesel only combustion and H_2-diesel fuel co-combustion with maximum H_2 concentration in the intake air (therefore at minimum diesel fuel condition). At a lower load of 3 bar IMEP, it can be observed from Fig. 6(a) that the duration of combustion increases significantly in the case of H_2-diesel fuel co-combustion relative to diesel fuel only combustion. At 3 bar IMEP, the in–cylinder H_2-air mixture is weaker than stoichiometric ($\varphi_H = 0.18$), and it suggested that this may result in the slower flame propagation speeds than the maximum speeds achievable during stoichiometric combustion. In contrast, with diesel fuel only ignition, an appreciable amount of diesel fuel-air mixture is already prepared during the delay period, and combusts rapidly, and close to TDC, following ignition, giving rise to higher rates of heat release [14,21]. At a higher load of 6 bar IMEP, where the in–cylinder H_2-air mixture is relatively close

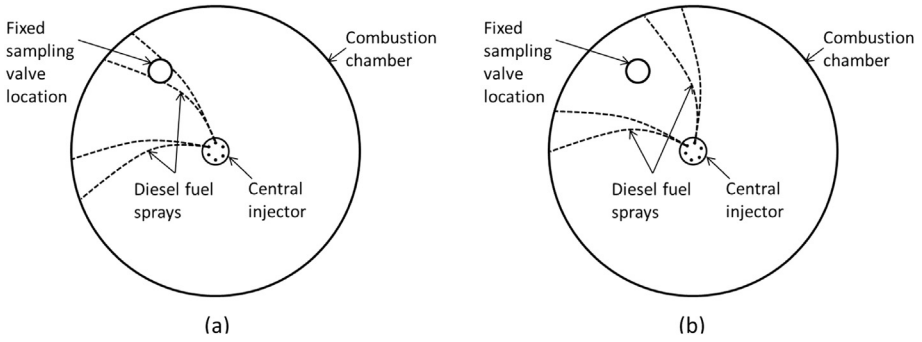

Fig. 5 – Schematic showing (a) sampling arrangement one and (b) sampling arrangement two relative to the diesel fuel sprays; changes to the position of the spray relative to the valve location was achieved by rotating the fuel injector.

to stoichiometric ($\varphi_H = 0.40$), both the duration of combustion and the peak rate of heat release (pHRR) for H_2-diesel fuel co-combustion are comparable to diesel fuel only combustion.

Fig. 6(b) shows the effect of H_2 addition on the ignition delay at various fixed diesel fuel injection periods. Throughout this paper, ignition delay is defined as the duration in CAD between the start of diesel fuel injection (SOI) and the start of combustion (SOC); SOI is taken to be the time (in CAD) at which the injector actuation current signal is sent, and SOC is taken as the time (in CAD) at which the first detectable incidence of heat release occurs from fuel burning. It can be seen from Fig. 6(b) that the addition of H_2 results in a general trend of increasing ignition delay, which reaches a peak and subsequently decreases with further H_2 addition. The increase in ignition delay could be attributed to the reduction in oxygen (O_2) concentration in the intake charge, as intake air O_2 is displaced by H_2 aspirated into the engine inlet manifold. The reduction in O_2 availability in the intake charge is expected to have led to a decrease in the rates of low temperature fuel reaction kinetics, that produce reactive radical species and escalate temperatures, thus delaying autoignition [14,19,20]. It is tentatively suggested that a further driver of the increased ignition delay with increasing H_2 addition may be an inhibiting influence of H_2 on the oxidation of diesel fuel. Fig. 6(b) shows the ignition delay trend reversing at higher engine loads (beyond ~4.5 bar IMEP), with the ignition delay decreasing with further addition of H_2. This trend reversal is believed to be due to, firstly, the elevated in–cylinder temperatures arising from higher engine loads which improve mixing rates of the injected liquid fuel; and secondly, as the H_2-air mixture ratio increases towards the stoichiometric level, the higher residual gas temperatures speed up the ignition reactions.

Table 4 – Gaseous sample extraction time CAD ATDC during the engine cycle and the corresponding sampling window in CAD.

Sampling instant (middle of sampling window) (CAD ATDC)	Duration of sampling window (CAD)	Diesel fuel injection period (μs)
10	6	325
25	10	325
40	15	325

Fig. 6(c) shows the effect of increasing H_2 addition, at various fixed diesel fuel injection periods, on the pHRR; the figure shows a general increase in the apparent peak heat release rates with increasing H_2 addition. For comparison purposes, Fig. 6(c) also shows the pHRR when the engine load is increased without any H_2 addition, that is, by merely increasing the amount of diesel fuel injected. It can be observed in Fig. 6(c) that the peak heat release rates for H_2-diesel fuel mixtures are generally lower than those for diesel fuel only. In addition to the discussion presented for Fig. 6(a), the retardation in the ignition delay (Fig. 6(b)) may also contribute to the reduction in pHRR with H_2-diesel fuel co-combustion relative to diesel fuel only combustion. As the duration of ignition delay increases the pHRR occurs further away from TDC, into the expansion stroke and this could be expected to result in higher energy losses through heat transfer.

Fig. 6(d) shows the indicated thermal efficiency of the engine at various fixed diesel fuel injection periods and engine loads. The indicated thermal efficiency was calculated as the ratio of the power output from the engine to the combined energy input from both diesel fuel and hydrogen. Comparing the indicated thermal efficiencies of diesel fuel only and H_2-diesel fuel mixtures, a small drop in the thermal efficiency is observed when H_2 is supplied to the engine. It is believed that the decrease in thermal efficiency with the addition of H_2, contrary to reports in the literature [6,7], could be due to some of the aspirated H_2 not burning in the engine cylinder and persisting into the exhaust [22]. As the amount of H_2 leaving the engine unburned was not measured, it was therefore not considered when calculating the indicated thermal efficiency (Fig. 6(d)), and is possible that the contradictory decrease in thermal efficiency may not have been observed had H_2 persisting into the exhaust been accounted for.

Gaseous emissions of CO, THC and CO_2

Fig. 7(a), (b) and (c) show the effect of H_2 addition, at various fixed diesel fuel injection periods, on the concentrations of CO, THC and CO_2 in the exhaust gas stream respectively. First, considering CO and THC (Fig. 7(a) and (b)), the concentrations of both these gases are high at low engine loads, but then rapidly decrease as the engine load (and level of H_2 addition) rises. At low loads, it is suggested that excessive dilution of

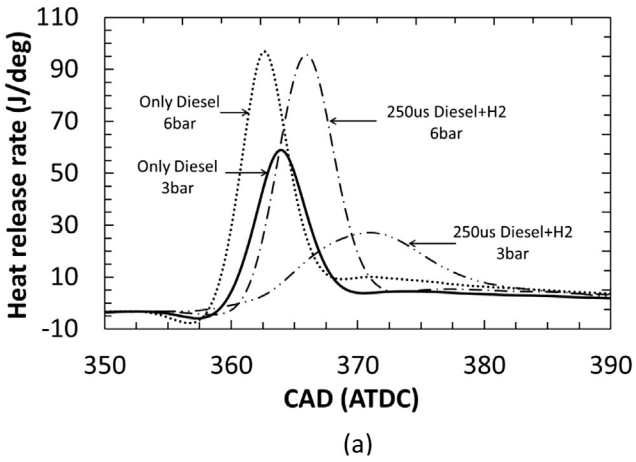

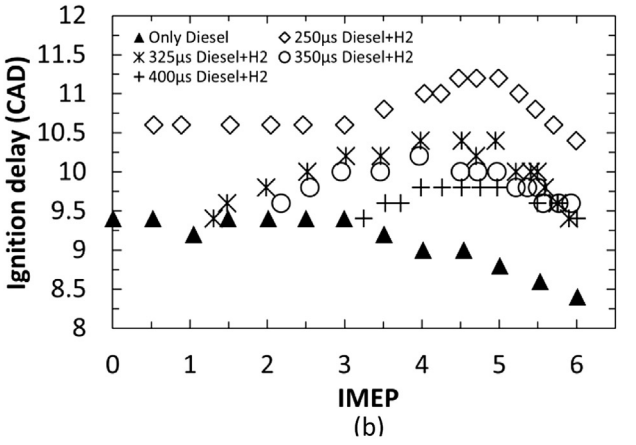

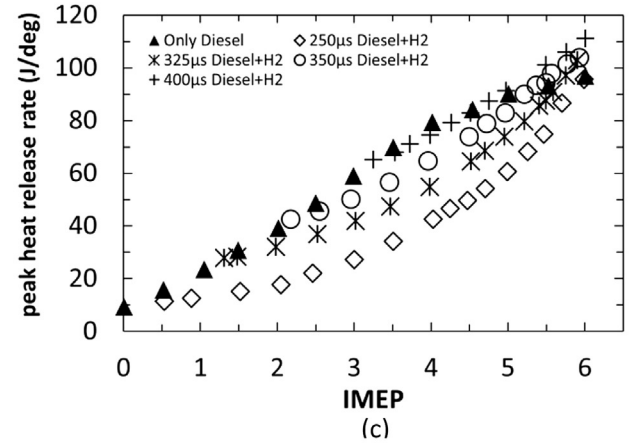

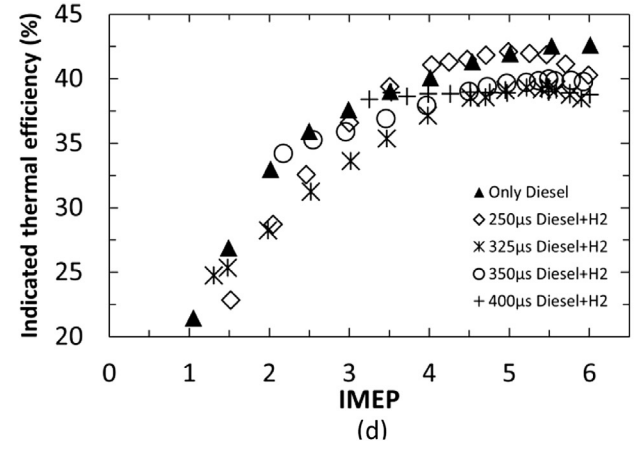

diesel fuel at the spray fringes, combined with lower in–cylinder gas temperatures, results in a diesel fuel-air mixtures which are leaner than their combustion limit, and fuel that is either unreacted or only partially oxidized. As the displacement of intake air by H_2 increases, and thereby the engine load rises, the diesel fuel-air mixture progressively strengthens towards stoichiometric levels, which when combined with high H_2 combustion temperatures, results in higher in–cylinder gas temperatures and more complete combustion.

Interestingly, Fig. 7(c) shows a gradual increase in the amount of CO_2 in the exhaust with an increasing amount of hydrogen addition, despite the fact that carbon flow rate to the combustion chamber is fixed (diesel fuel injection duration in µs is fixed). The addition of H_2 in the intake manifold displaces some of the intake air, therefore reducing the flow rate of air through the engine. The H_2 aspirated with the intake air is oxidized to water vapour in the exhaust, which is condensed by the emissions analyser rack prior to measurement of CO_2 in the exhaust gas, therefore reducing the flow rate of exhaust gas. Since the carbon flow rate to the engine is fixed, the amount of CO_2 produced by the diesel fuel could be expected to remain consistent. Therefore, it is suggested that the observed increase in the concentration of CO_2 in the exhaust gas (Fig. 7(c)) is a consequence of the reduced exhaust flow rate. A secondary, although less significant, possible reason for the increase in CO_2 emissions could potentially be a slight increase in the combustion efficiency of diesel fuel as H_2 addition increases, as an effect of increasing in–cylinder gas temperatures (as suggested by the higher pHRR with H_2 addition observed in Fig. 6(c)). There is some evidence for this in the results in Fig. 7(a) and (b) which show a decrease in exhaust gas carbon monoxide and unburned hydrocarbon emissions respectively, with the addition of H_2.

Fig. 7(b) also shows that the concentrations of the unburned hydrocarbon exhaust emissions, at different H_2-diesel mixtures, tend to converge at 6 bar IMEP, suggesting almost complete oxidation of all the available hydrocarbon fuel. The remaining hydrocarbons which persist to the exhaust could be originating from a number of sources; crevices in the piston and rings, desorbed off the thin oil layer covering the cylinder walls or from the vaporization of fuel from the injector nozzle sac volume late in the engine cycle [14].

NO_x emissions

Fig. 8(a) shows the concentration of NO_x in the engine exhaust with increasing amounts of H_2 supplied to the engine (at various fixed diesel fuel injection periods). Fig. 8(a) shows that when the diesel fuel was limited to the bare minimum (250 µs), just sufficient to pilot-ignite the hydrogen, then at low engine loads of up to 4 bar IMEP, very little NO_x (around 20 ppm) was formed. The exhaust NO_x levels, however, increased rapidly

Fig. 6 – (a) Heat release rate curves and combustion characteristics (b) duration of ignition delay, (c) apparent net peak heat release rates (J/deg) and (d) indicated thermal efficiency of the engine at various engine loads and H_2-diesel fuel proportions.

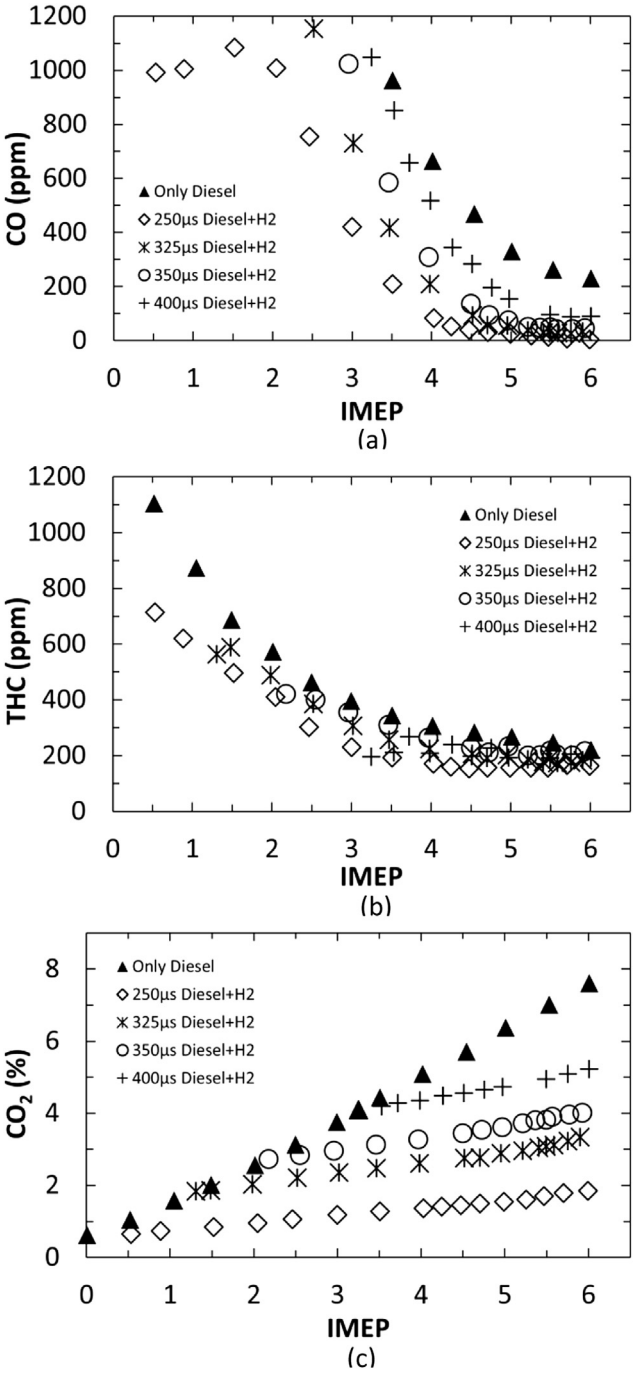

Fig. 7 – Variation in exhaust emissions of (a) carbon monoxide (CO), (b) unburned total hydrocarbons (THC) and (c) carbon dioxide (CO_2) at various engine loads and H_2-diesel fuel proportions.

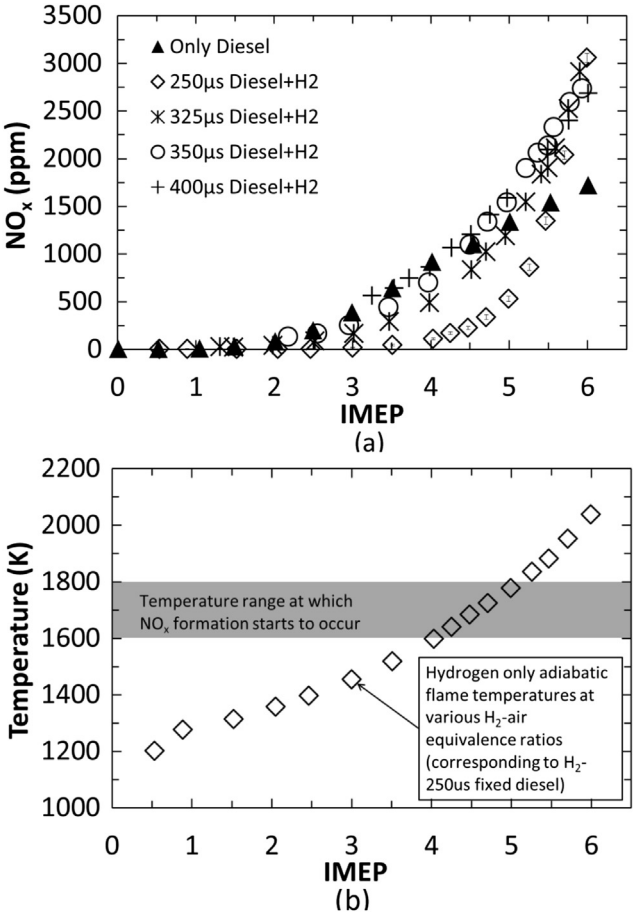

Fig. 8 – Variation in (a) exhaust emissions of nitrogen oxides (NO_x) and (b) adiabatic flame temperatures at various engine loads and H_2-diesel fuel proportions. The temperatures were calculated using GASEQ software at an initial pressure of 40 bar and initial temperature of 600 K.

when the engine load rose beyond 4 bar IMEP (Fig. 8(a)). This suggests that at lower engine loads below 4 bar IMEP, the H_2-air mixture was far too lean for NO_x to form, with the resulting combustion temperatures from H_2 combustion remaining below the temperatures which promote rapid thermal NO_x formation. At engine loads above 4 bar IMEP, the H_2 concentration in the intake air became sufficient for the in–cylinder gas temperatures to reach a level at which the kinetically controlled NO_x formation rates accelerated significantly, resulting in substantial exhaust emissions of NO_x (Fig. 8(a)).

Fig. 8(b) helps explain the test results presented in Fig. 8(a). In general, the principal reactions governing the oxidation of molecular nitrogen to NO_x initiate at temperatures ranging between 1600 K and 1800 K [14] as shown in Fig. 8(b). Fig. 8(b) shows that with the level of addition of H_2 present between 1 and 4 bar IMEP, the H_2-air mixture was still too lean and the hydrogen adiabatic flame temperature was below that needed for significant quantities of NO_x to be produced. It can be seen that only when levels of H_2 addition reached those required to produce an engine load of greater than 4 bar IMEP, was the H_2 adiabatic flame temperature sufficient for NO_x production (Fig. 8(b)), coinciding with the sharp increase in NO_x emissions observed in Fig. 8(a).

An additional observation from Fig. 8(a) is that diesel fuel was also a significant source of NO_x formation. This is related to the fact that combustion of diesel sprays can be expected to always occur at close-to-stoichiometric conditions at the fuel spray fringes with resultant local temperatures high enough for NO_x formation [23]. At higher loads of 5.5 bar IMEP and above, and with diesel fuel injection duration of 250 µs, it is

apparent that NO_x emissions produced during H_2-diesel fuel co-combustion increase above the level of NO_x observed in the case of diesel fuel only combustion. It is suggested that this may be attributable to higher in–cylinder gas temperatures in the case of combined H_2-diesel fuel co-combustion than in diesel only combustion, resulting in higher rates of NO_x formation.

To further explain the effect of H_2-air mixture stoichiometry on NO_x emissions, the data in Fig. 8(b) has been re-plotted in Fig. 9. Each curve on Fig. 9 corresponds to a constant engine load (IMEP) and shows the variations in exhaust NO_x emissions when a constant engine load is obtained at different combinations of H_2-air mixture ratios by the substitution of diesel fuel with H_2.

Referring to Fig. 9, consider first the NO_x emissions at a lower constant engine load of 4 bar IMEP. Fig. 9 shows that at 4 bar IMEP, an increase in the H_2-air equivalence ratio (φ_H) resulted in reduced NO_x emissions. This is a particularly interesting result and can be explained as follows. At 4 bar IMEP, the H_2-air equivalence ratio is too lean to produce NO_x (Fig. 8(a) and (b)). The bulk of NO_x emissions come from diesel fuel combustion. The diesel fuel injected into the combustion chamber of the diesel engine used in this study can always be expected to produce significant quantities of NO_x, because spray combustion takes place around the spray fringe where the diesel fuel-air equivalence ratio is at about stoichiometric value. Therefore, the gradual substitution of diesel fuel by H_2 (at constant engine loads of less than or equal to 4 bar IMEP) resulted in the gradual reduction of NO_x exhaust emissions.

At a higher engine load of 6 bar IMEP, a different picture emerges (Fig. 9). The substitution of diesel fuel by H_2 does not result in a reduction in NO_x but, instead, in a monotonic increase in NO_x. At this engine load, the amount of diesel fuel injected is relatively large and H_2 addition has no effect in reducing NO_x, despite the fact that diesel fuel is being substituted by H_2. It appears that at these higher loads, H_2 enhances the production of NO_x by further raising the temperatures in the diesel fuel spray combustion zones. As the substitution of diesel fuel with H_2 increases at a constant engine load of 6 bar IMEP, the amount of H_2 needed to sustain the 6 bar IMEP becomes high (φ_H reaches 0.4), which raises the in–cylinder gas temperature above the thermal NO_x production temperature (Fig. 8(b)).

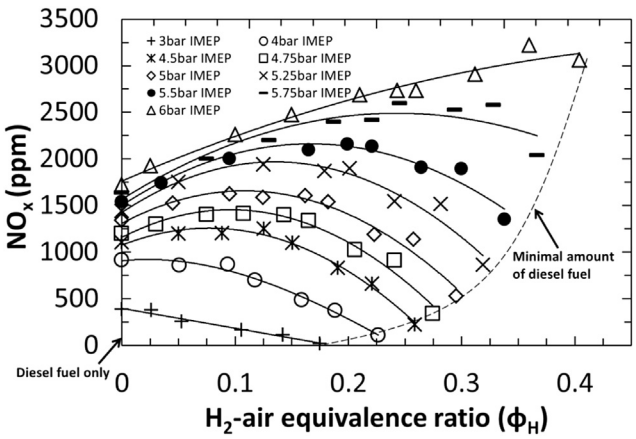

Fig. 9 – Exhaust emissions of nitrogen oxides (NO_x) at constant engine loads and variable H_2-air equivalence ratio (φ_H).

Consider now a relatively intermediate engine load of 5 bar IMEP (Fig. 9). Fig. 9 shows that, at this constant load, NO_x first increases with the substitution of diesel fuel by H_2, but then as H_2 substitution becomes higher, NO_x begins to fall. A likely explanation for this observation can be the following. At low H_2 substitution levels, the diesel fuel combustion provides numerous ignition sites and the bulk of the energy release. Therefore NO_x production would be dominated by the diesel fuel burning at near-stoichiometric local sites and the H_2 providing, locally, additional synergetic heat release and temperature rise, resulting in extra NO_x formation. With the progressive removal of diesel fuel and substitution with H_2 there comes a point when the amount of diesel fuel removed is large enough for the high rate of NO_x production from diesel fuel to be curtailed. At the same time, NO_x production from H_2 is not significant, because at intermediate engine loads the H_2-air equivalence ratio is still not sufficiently high for commensurate NO_x production, at the same levels that was produced by the diesel fuel that the H_2 substituted. Hence a drop in exhaust NO_x emissions is observed (Fig. 9).

Nitrogen dilution experiments

For all the experiments presented in this paper the H_2 was aspirated into the engine inlet manifold, thus displacing some of the intake air with hydrogen. While the H_2 takes part in the combustion process and releases energy which in turn raises the local gas temperatures in the engine cylinder and thereby, increases NO_x formation rates, the H_2 also has an additional effect of diluting the local amount of air, and the decreasing oxygen availability could be expected to reduce NO_x. This effect of H_2 addition to reduce NO_x may partially offset the increased NO_x production due to higher in–cylinder temperatures brought about as a result of H_2 combustion. In an effort to separate and quantify the dilution effect of H_2 on NO_x levels, the intake air was displaced by nitrogen (rather than H_2) to an equal volume flow rate as when using H_2 in the intake. The nitrogen (N_2) dilution tests were conducted at two constant engine loads, 4 bar and 6 bar IMEP.

Fig. 10 shows the results of the N_2 dilution experiments. It can be seen from Fig. 10 that at the low engine load of 4 bar IMEP, a similar effect of H_2 and N_2 addition is observed, with NO_x levels decreasing with increasing levels of either gas. It implies that both gases act just as diluents, by reducing the amount of O_2 and, thereby, reducing NO_x formation from the diesel fuel spray. This result is consistent with previous results presented in this paper which showed that at an engine load of 4 bar IMEP, the H_2-air mixture is too lean to result in the necessary temperature rise for production of significant levels of NO_x. However, it must be noted that with increasing H_2 addition, the diesel fuel flow rate has to be reduced in order to maintain a constant engine load. Since diesel fuel can be expected to produce significant NO_x at these conditions (Fig. 8(a)), it is difficult to discern whether the reduction in NO_x emissions is due to the reduction in diesel fuel or the diesel fuel being replaced by a lean H_2-air mixture.

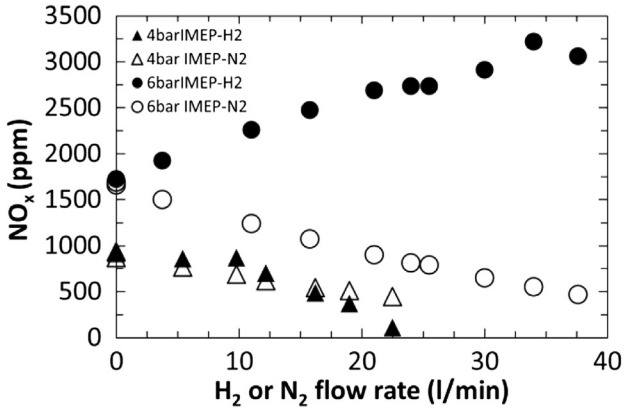

Fig. 10 – Exhaust emissions of NO_x at constant engine loads and varying H_2 and N_2 flow rates.

At 6 bar IMEP, the N_2 dilution causes an appreciable reduction in the NO_x produced from the diesel fuel spray. However, with H_2 addition at the constant load of 6 bar IMEP, the combustion of H_2 produces significantly high temperatures which result not only in offsetting the dilution effect on NO_x production, but also in a monotonic rise in NO_x as the H_2-air equivalence ratio is gradually increased by means of substitution of diesel fuel with hydrogen. It must however be remembered that.

Particulate emissions

Fig. 11 shows the exhaust emissions of total particulate mass at various fixed diesel fuel injection periods and engine loads. The change in engine load was achieved by varying the amount of H_2 addition, while keeping the diesel fuel supplied to the engine fixed. At a fixed diesel fuel injection period, it can be seen that increasing H_2 addition results in a decrease in PM emissions up to 5.5 bar IMEP. At a low fixed diesel fuel injection period, such as 250 μs, particulate emissions drop to negligible levels as H_2 is introduced into the engine. Increasing engine loads beyond 5.5 bar IMEP results in a small increase in emissions of PM (Fig. 11). The introduction of H_2 in the intake charge can be expected to have resulted in two competing effects on PM formation. Firstly, it can be expected that the reduction in O_2 availability due to the displacement of intake air with H_2 accelerated particle formation via rising pyrolysis rates and, secondly, the high temperatures resulting from H_2 combustion led to a counteracting increase in the rate of thermal soot oxidation. Particulates are mostly formed in the fuel rich, and highly oxygen deficient, core regions of the diesel fuel spray, within the spray flame envelope, when the fuel vapour comes in contact with the hot burned gases [14,24]. Oxidation of these particulates occurs with the continuous breakdown of the spray due to intense turbulence levels and mixing with air, when PM oxidizes to form gaseous products such as CO and CO_2. The eventual level of PM emissions in the exhaust depends on the balance between these two competing effects, formation and oxidation. Fig. 11 suggests that the enhanced oxidation process prevails over increased pyrolysis rates when H_2 supply to the engine is increased, resulting in an overall reduction in PM emissions at fixed diesel fuel injection periods.

Fig. 12 shows the percentage reduction in the total particulate mass plotted against the percentage reduction in fuel carbon supplied to the engine, at constant engine loads. The reduction in fuel carbon was achieved by lowering the amount of diesel injected and the loss in engine power was restored by adding H_2 in order to maintain a constant engine load. The percentage reductions in both particulates and fuel carbon were calculated against the values obtained with the engine operating on only diesel fuel (no H_2 addition). The 1:1 dashed diagonal line in Fig. 12 represents equivalent reductions in both PM emissions and fuel carbon supplied to the engine.

For engine loads below 4 bar IMEP, Fig. 12 shows the reductions in PM emissions to lie in the top half of the graph (above the 1:1 dashed line), implying a beneficial effect of H_2 addition on PM reduction beyond simple fuel carbon displacement. For example, at a constant engine load 3 bar IMEP, a 10% reduction in fuel carbon causes up to 50% reduction in particulate matter. Therefore, as previously discussed, it could be suggested that an increase in H_2-air stoichiometry (or a decrease in diesel fuel) promotes soot

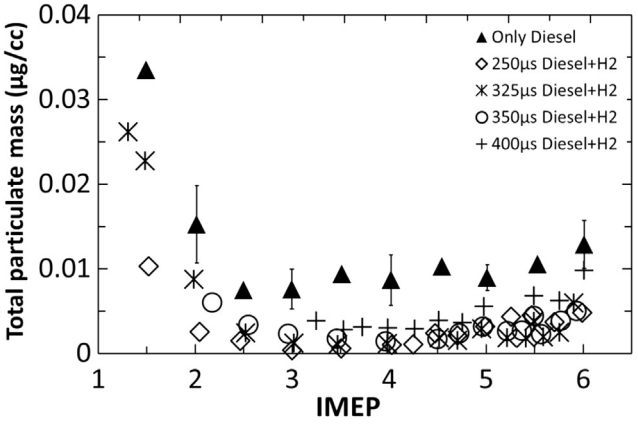

Fig. 11 – Variation in exhaust emissions of total particulate mass (μg/cc) at various engine loads and H_2-diesel fuel proportions.

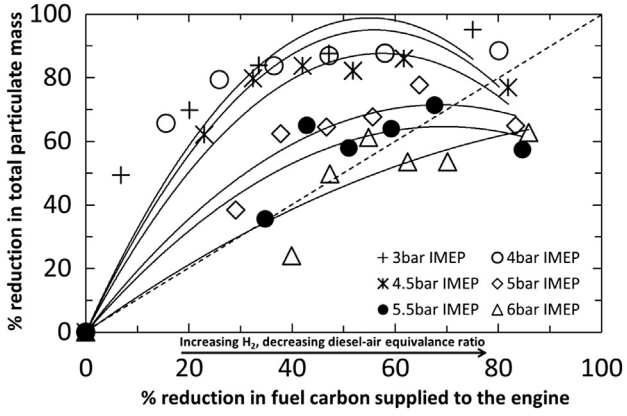

Fig. 12 – Comparison of the percentage reduction in total particulate mass with percentage reduction in the carbon content of the combustible mixture at constant engine loads.

oxidation, or reduces initial soot formation, and at low engine loads these effects are more important than any increase in soot formation due to O_2 reduction. At the higher engine load of 5 bar IMEP, Fig. 12 shows that the effect of H_2 substitution for diesel fuel results in a net reduction in PM, but this effect is less than that at the lower load of 3 bar IMEP.

At the maximum load tested of 6 bar IMEP (Fig. 12), the reductions in particulate mass lie almost entirely in the bottom half of the graph (below the 1:1 dashed line). This suggests that the addition of H_2 results in only a small reduction in PM, with this reduction being smaller that the reduction in PM that could be expected from merely the drop in fuel carbon supplied to the engine. One possible explanation for this is, at higher engine loads (6 bar IMEP or above) the air displaced due to the addition of substantial quantities of H_2 to the engine severely affects the oxygen availability for PM oxidation, despite the increase in in–cylinder temperatures arising from higher H_2-air equivalence ratios.

In–cylinder gas sample analysis

This section of the paper presents the results of in–cylinder gas sampling with the two sampling arrangements (in the spray core and between two sprays), as discussed in Section Experimental set 2: in–cylinder gas sampling tests.

Fig. 13(a) and (b) show, respectively, the concentrations of unburned total hydrocarbons and particulate matter in gas samples at various engine loads extracted from the engine cylinder at 10, 25 and 40 CAD ATDC of the combustion cycle with the two in–cylinder sampling arrangements relative to the diesel fuel sprays (Fig. 5). The tests were conducted at a fixed diesel injection period of 325 μs and the increase in engine load was achieved by adding H_2 to the intake charge. Fig. 13(a) and (b) show that the concentrations of total hydrocarbons and particulate matter when sampling within the fuel spray were higher, at all engine loads, compared to the results obtained when sampling between two fuel sprays. In the fuel dense core of the diesel spray, local average equivalence ratios are rich, due to lack of air entrainment, especially during the initial stages of combustion, and thereby generate high particulate concentrations. The region in between two individual diesel sprays contains relatively low amounts of fuel vapour that have been swept around by the swirling air flow, and hence is characterized by leaner diesel fuel equivalence ratios, leading to more complete combustion and lower THC and PM concentrations. These observations are in agreement with similar gas sampling studies undertaken so as to map out fuel distribution in diesel engine cylinders [25–27].

It can also be observed from Fig. 13(a) and (b) that the concentrations of THC and PM, respectively, generally decreased as combustion proceeded; this can possibly be attributed to the enhanced mixing of diesel fuel and air as spray was broken up and came into contact with hot unburned gases, resulting in more complete diesel fuel oxidation.

The generally decreasing levels of THC and PM emissions with increasing engine load (IMEP), observed at the three sampling instants (Fig. 13(a) and (b)), are in agreement with the measurements of exhaust gas composition discussed in Section Gaseous emissions of CO, THC and CO_2. H_2 addition is expected to have potentially increased diesel combustion efficiency by raising the in–cylinder gas temperatures, thereby promoting the rate of thermal soot oxidation.

Fig. 13(c) shows the molar fraction of CO_2 in gas samples at various engine loads extracted from the engine cylinder at 10, 25 and 40 CAD ATDC of the combustion cycle with the two in–cylinder sampling arrangements relative to the diesel fuel sprays (Fig. 5). At 10 CAD ATDC the CO_2 concentrations were quite similar between the two sampling arrangements, at all the engine loads. As combustion progressed, the CO_2 concentrations in spray core remained fairly high, whereas the CO_2 levels in the gas samples obtained from between two sprays decreased. At 40 CAD ATDC, the CO_2 concentrations with both the sampling arrangements fell as the burned gas products became further diluted with the unreacted intake air that moves from within the piston bowl to the region above the piston as the expansion stroke progresses.

As with the exhaust CO_2 emissions (Fig. 7(c)), the CO_2 concentrations in the in–cylinder gas samples, at all sampling instants, gradually increased with increasing H_2 addition (increasing IMEP) (Fig. 13(c)), the reasons for which have been discussed in detail in Section Gaseous emissions of CO, THC and CO_2.

Fig. 13(d) shows the NO_x concentrations in gas samples at various engine loads extracted from the engine cylinder at 10, 25 and 40 CAD ATDC of the combustion cycle with the two in–cylinder sampling arrangements relative to the diesel fuel sprays (Fig. 5). At 10 and 25 CAD ATDC and at all engine loads, NO_x concentrations were higher between the two sprays, as compared to those in the spray core. Comparing the NO_x concentrations between 10 and 25 CAD ATDC, an increase was seen in NO_x in the spray core, while, between the two sprays, NO_x remained quite similar at both sampling instants (10 and 25 CAD ATDC). At a later stage of the engine cycle, at 40 CAD ATDC, the NO_x concentrations with both sampling arrangements were of similar magnitude. However, with both sampling arrangements, NO_x concentrations at 40 CAD ATDC were lower compared to those at 25 CAD ATDC.

Spatial and temporal distribution of in–cylinder NO_x and CO_2

From the in–cylinder sampling results presented in Fig. 13, and notwithstanding that some relative movement of the diesel spray between the three sampling times could be expected due to the effects of in–cylinder swirl, the following further discussion is made. Air is entrained into the diesel fuel vapour at the periphery of the dense diesel fuel spray core by the swirling motion of the air; this, combined with the turbulent environment inside the chamber, results in the mixing and dilution of fuel vapour mixing in the intake charge, especially in the regions between the individual sprays, where there is a higher initial concentration of the air and hydrogen intake mixture [23]. As mentioned previously, it can be expected that autoignition first occurs at these close-to-stoichiometric diesel fuel vapour-air pockets around the fuel sprays and results in the rapid burning of both the premixed diesel vapour and H_2-air mixtures around the diesel fuel ignition sites. As suggested in Section NO_x emissions, the temperature increase resulting from H_2 combustion adds to the diesel flame temperature, and NO_x production initiates when these combined temperatures exceed that required for thermal NO_x formation. Considering

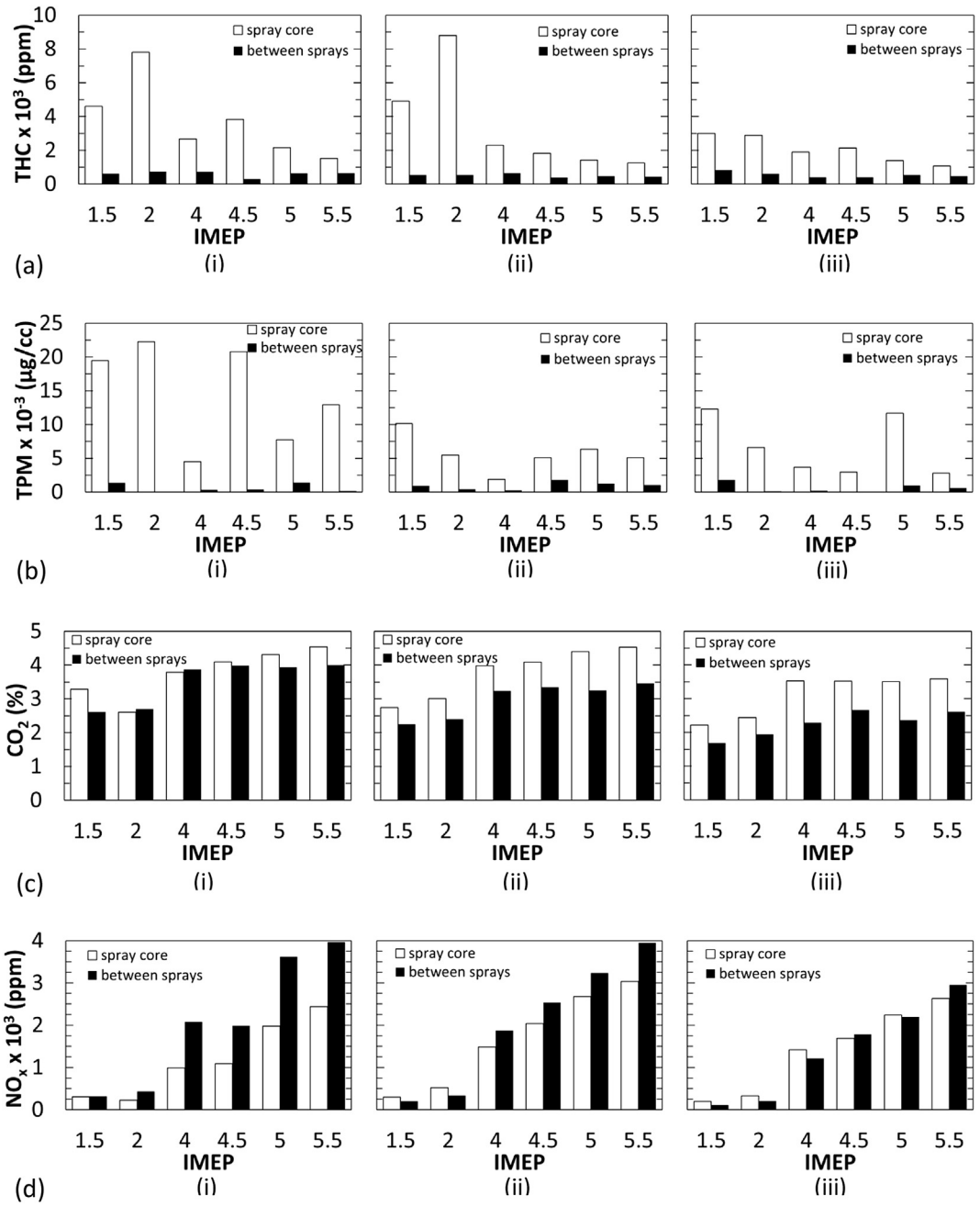

Fig. 13 – Measurement of (a) in–cylinder unburned total hydrocarbon (THC) concentration, (b) total particulate mass (TPM), (c) carbon dioxide (CO_2) concentration and (d) nitrogen oxide (NO_x) concentration in gas samples collected at (i) 10 CAD, (ii) 25 CAD and (iii) 40 CAD ATDC at fixed diesel with increasing amounts of H_2 and variable engine loads (at engine speed 1200 rpm) with two sampling arrangements (Fig. 5).

the difference in the concentrations of NO_x with the two sampling arrangements at 10 CAD ATDC (Fig. 13(d), (i)), the region in between two sprays (arrangement two) could be expected to have a higher H_2-air concentration resulting in higher gas temperatures and, therefore, higher NO_x formation rates. On the other hand, the lower NO_x concentrations in the spray core (at 10 CAD ATDC) could be attributable to the relatively low concentration of air in the fuel rich core of the diesel fuel spray, resulting in lower combustion temperatures and, hence, reduced NO_x formation. Furthermore, some of the energy released in this fuel rich region can be expected to have been absorbed for fuel pyrolysis [14], resulting in lower gas temperatures and NO_x formation rates.

Considering the increase in NO_x concentrations between 10 and 25 CAD ATDC (Fig. 13(d)), in the spray core, the rich diesel spray core might be expected to have broken up, as combustion progressed, with the H_2-air mixture being rapidly entrained into the disintegrated diesel fuel spray. The combined fuel mixture is expected to have burned at sufficiently high temperatures to increase NO_x formation rates as combustion

progressed from 10 to 25 CAD ATDC. This is further reinforced by the appreciable CO_2 concentrations observed in the spray core at 25 CAD ATDC, suggesting considerable combustion of carbon-containing fuel occurring at that location (Fig. 13(c)).

Considering now the region between the two sprays, the NO_x concentration showed no significant change, between 10 and 25 CAD ATDC (Fig. 13(d)), as the engine expansion stroke had commenced and the mixing of the post-combustion gases with excess air could be expected to have frozen the NO_x formation reactions [28]. A decrease in CO_2 concentrations was observed from 10 to 25 CAD ATDC (Fig. 13(c)), between the sprays. For example, at 4 bar IMEP, CO_2 concentrations, between the sprays, decreased from about 4% to 3% as combustion progressed from 10 to 25 CAD ATDC. This could be attributable to the mixing of CO_2 with excess air, resulting in a reduction in the CO_2 concentration measured in the sampled in–cylinder gas. At 40 CAD ATDC, CO_2 (Fig. 13(c)) and NO_x (Fig. 13(d)) concentrations in the extracted sample were quite similar, with both sampling arrangements. This may be expected, as at later stages of combustion the effects of air swirl and reverse squish flow [14,15] promoted the redistribution of in–cylinder gaseous composition, creating near homogenous conditions in the cylinder.

Conclusions

1. An increase in the duration of ignition delay was observed at intermediate engine loads with H_2 addition, which could be attributed to the decreasing O_2 concentration in the intake charge. This reduction in O_2 availability can be expected to lead to a reduction in the rate of low temperature fuel reaction kinetics, delaying autoignition. At high engine loads, the ignition delay period was observed to have reduced in duration, as elevated in–cylinder temperatures improved the evaporation and subsequent mixing of the injected fuel with air.
2. An increase in CO_2 emissions (both exhaust and in–cylinder) with H_2 addition was observed despite fixed fuel carbon flow rate into the combustion chamber (diesel fuel injection period was fixed). The displacement of intake air by H_2 and the subsequent oxidation of H_2 to water vapour reduced the exhaust flow rate, since the water vapour is condensed by the analysers prior to CO_2 measurement. Except for a small increase in diesel combustion efficiency (as seen by the decrease in exhaust gas carbon monoxide and unburned hydrocarbon emissions), the CO_2 produced by the diesel fuel is expected to be unchanged and the CO_2 concentration in the exhaust can be expected to rise, as a consequence of the reduced exhaust flow rate.
3. NO_x emissions (both exhaust and in–cylinder) were observed to increase very rapidly with the addition of H_2 but only when the combined temperatures resulting from H_2-diesel fuel co-combustion exceeded the threshold temperature for NO_x formation temperatures.
4. At fixed diesel fuel injection periods and engine loads below 5.5 bar IMEP, a reduction in the overall PM emissions was observed with H_2 addition, as soot burnout by thermal oxidation offset the effects of soot formation via pyrolysis. At higher engine loads, the effect of dilution of intake O_2 due to displacement by H_2 becomes the primary influence on particulate matter generation and a small rise in PM emissions was observed.
5. At low engine loads, the addition of H_2 promoted soot burnout due to elevated temperatures and higher oxidation rates; at intermediate engine loads, the effects of soot formation and oxidation counterbalanced each other; and at high engine loads, the excessive displacement of intake O_2 by H_2 led to slightly increased rates of soot formation.
6. From in–cylinder gas sampling results it was observed that at early stages of combustion (10 CAD ATDC), NO_x concentrations within the diesel fuel spray were lower than those measured in between two individual fuel sprays. This could be attributed to a higher concentration of H_2-air mixture burning in between the sprays, combined with the combustion of significant amounts of diesel fuel vapour occurring between the sprays. This is expected to have resulted in high temperatures in this region (between he sprays) and, therefore, higher NO_x formation rates in comparison to the NO_x formation rates within the spray, where a deficiency of air existed.

Nomenclature

ATDC	after-top-dead-centre
atm	standard atmosphere
BTDC	before-top-dead-centre
CAD	crank angle degree
cc	cubic centimetre
CFD	computational fluid dynamics
CI	compression ignition
CO	carbon monoxide
CO_2	carbon dioxide
H_2	hydrogen
HO_2	hydroperoxyl
IMEP	indicated mean effective pressures
NO	nitric oxide
NO_2	nitrogen dioxide
NO_x	nitrogen oxides
O_2	oxygen
OH	hydroxyl
PM	particulate matter
ppm	parts per million
ppr	pulses per revolution
SOC	start of combustion
SOI	start of injection
TDC	top-dead-centre
THC	total hydrocarbons
φ_D	diesel-air equivalence ratio
φ_H	hydrogen-air equivalence ratio

REFERENCES

[1] Tsolakis A, Hernandez J. Dual fuel diesel engine operation using H_2. Effect on particulate emissions. Energy & Fuels 2005:418–25.

[2] Karim G. Hydrogen as a spark ignition engine fuel. Int J Hydrogen Energy 2003;56:256–63.
[3] Lambe S, Watson H. Optimizing the design of a hydrogen engine with pilot diesel fuel ignition. Int J Veh Des 1993;14:370–89.
[4] Lilik G, Zhang H, Herreros J. Hydrogen assisted diesel combustion. Int J Hydrogen Energy 2010;35:4382–98.
[5] Saravanan N, Nagarajan G. Combustion analysis on a DI diesel engine with hydrogen in dual fuel mode. Fuel 2008;87:3591–9.
[6] Masood M, Ishrat M, Reddy A. Computational combustion and emission analysis of hydrogen–diesel blends with experimental verification. Int J Hydrogen Energy 2007;32:2539–47.
[7] Christodoulou F, Megaritis A. Experimental investigation of the effects of separate hydrogen and nitrogen addition on the emissions and combustion of a diesel engine. Int J Hydrogen Energy 2013;38:10126–40.
[8] Varde K, Varde L. Reduction of soot in diesel combustion with hydrogen and different H/C gaseous fuels. In: 5th world hydrogen energy, Toronto, Canada; 1984.
[9] Saravanan N, Nagarajan G. An experimental investigation of hydrogen-enriched air induction in a diesel engine system. Int J Hydrogen Energy 2008;33:1769–75.
[10] Tomita E, Kawahara N, Piao Z, Fujita S, Hamamoto Y. *Hydrogen combustion and exhaust emissions ignited with diesel oil in a dual fuel engine*. SAE Pap 2001:2001–01–3503.
[11] Brunt MFJ, Rai H, Emtage AL. *The calculation of heat release energy from engine cylinder pressure data*. SAE Pap 1998:981052.
[12] Naber J. Hydrogen combustion under diesel engine conditions. Int J Hydrogen Energy 1998;23:363–71.
[13] Masood M, Ishrat MM. Computer simulation of hydrogen–diesel dual fuel exhaust gas emissions with experimental verification. Fuel 2008;87:1372–8.
[14] Heywood JB. Internal combustion engine fundamentals. 1st ed. New York: McGraw-Hill; 1988.
[15] Zhao H, Lowry G, Ladommatos N. *Time-resolved measurements and analysis of in-cylinder gases and particulates in compression-ignition engines*. SAE Pap 1996:961168.
[16] Tsurushima T, Shimazaki N, Asaumi Y. Gas sampling analysis of combustion processes in a homogeneous charge compression ignition engine. Int J Engine Res 2000;1:337–52.
[17] Nowak L, Guibert P, Cavadias S, Dupré S, Momique JC. Methodology development of a time-resolved in-cylinder fuel oxidation analysis: homogeneous charge compression ignition combustion study application. Combust Flame 2008;154:462–72.
[18] Zhao H, Ladommatos N. Engine combustion instrumentation and diagnostics. Society of Automotive Engineers; 2001.
[19] Westbrook CK. Chemical kinetics of hydrocarbon ignition in practical combustion systems. Proc Combust Inst 2000;28:1563–77.
[20] Andree A, Pachernegg SJ. *Ignition conditions in diesel engines*. SAE Pap 1969:690253.
[21] Hellier P, Ladommatos N, Allan R, Payne M, Rogerson J. The impact of saturated and unsaturated fuel molecules on diesel combustion and exhaust emissions; 2011. 2011–01–1922.
[22] Gatts T, Li H, Liew C, Liu S, Spencer T, Wayne S, et al. An experimental investigation of H_2 emissions of a 2004 heavy-duty diesel engine supplemented with H_2. Int J Hydrogen Energy 2010;35:11349–56.
[23] Dec JE. *A conceptual model of di diesel combustion based on laser-sheet imaging*. SAE Pap 1997:970873.
[24] Ning M, Vuan-Xian Z, Zhen-Huan S, Guo-dong H. *Soot formation, oxidation and its mechanism in different combustion systems and smoke emission pattern in DI diesel engines*. SAE Pap 1991:910230.
[25] Nightingale DR. *A fundamental investigation into the problem of no formation in diesel engines*. SAE Pap 1975:750848.
[26] Bennethum JE, Mattavi JN, Toepel RR. *Diesel combustion chamber sampling – hardware, procedures, and data interpretation*. SAE Pap 1975:750849.
[27] Rhee KT, Myers PS, Uyehara OA. *Time- and space- resolved species determination in diesel combustion using continuous flow gas sampling*. SAE Pap 1978:780226.
[28] Stone R. Introduction to internal combustion engines. 4th ed. New York: Palgrave Macmillan Limited; 2012.